Travelling wave solution of shock structure in an unsteady flow of a viscous non-ideal gas

Manoj Singh & Arvind Patel[1]

Department of Mathematics,
University of Delhi,
Delhi 110 007, India

smanojs2du@gmail.com & apatel@maths.du.ac.in

Abstract

The structure of shock wave in one-dimensional unsteady flow of a viscous non-ideal gas between the two uniform boundary states is investigated by the method of travelling wave solution. The system of basic gas dynamic equations are reduced into a single ordinary differential equation of first order for non-dimensional velocity. The exact solution for velocity, pressure, temperature and change in entropy are obtained between the boundary states. It has been found that there exist a travelling shock transition zone of the thickness of order 10^{-6} meter. The shock structure depends on Mach number, viscosity, adiabatic exponent and non-idealness of the gas.

Subject Classification: 76L05, 76N15, 80A17
Keywords: Shock wave, Navier-Stokes equations, Non-ideal gas, Viscosity.

1 Introduction

Travelling wave solution has been extensively used in the solution of many physical problems. Such solutions were first considered in 1930s by Fisher[1] and Kolmogorov, Petrovsky, and Piscounoff [2] for what has now known as the Fisher-KPP equation. Travelling wave solutions of reaction-diffusion equations have been extensively covered in [3]. Travelling wave solutions of a non-linear reaction-diffusion equations in chemotaxis model for bacterial pattern formation was studied by Mamsour [4]. Traveling shock waves arising in a model of malignant invasion was studied by Marchant, Norbury and Perumpanani [5]. Traveling wave phenomena for viscoelastic generalization of Burger's equation was presented by Camacho, Guy and Jacobsen [6]. Recently in 2015, Eabay and Sengul [7] have given travelling waves in one-dimensional non-linear models of strain-limiting viscoelasticity.

The study of structure of shock wave is important due to the need of development of a consistent theory which is valid under experimental measurement and is equally true up to the scale of molecular mean free path. It has been a challenging field of investigation for theoreticians and experimental scientist for a long time. Shock wave is a narrow transition

[1] corresponding author

zone (order of mean free path) in gas flow between the supersonic upstream and subsonic downstream. The internal structure of shock wave is to study the rapid change of flow variables such as velocity, pressure, temperature, change in entropy, viscous stress, heat flux, shock asymmetry and ratio of mean free path with the thickness of shock wave etc, through a narrow region between two uniform state. The reason behind the special interest to the shock structure problem is to study the discontinuity in the fluid flow in a narrow region of the order of mean free path under the objection on the validity of continuum model.

There are a rich history of theoretical and experimental study of shock wave structure. The theoretical treatment of shock structure is based either on continuum model or Navier-Stokes Fourier's equations, or on kinetic theory model ie analytical/numerical solutions of Boltzmann equation. In the treatment of this problem, by the equations of fluid mechanics, Rankine [8], Rayleigh [9] and Taylor [10] had recognized that the effect of the viscosity and heat conduction must be taken into account. Becker [11], Thomas [12], [13], Morduchow and Libby [14], Gilberg and Paolucci [15] were the early investigator for shock structure in ideal gas under presence or absence of viscosity and heat conduction. In 1984, Khidr and Mohmoud [16] have studied shock wave structure for arbitrary Prandtl numbers and high Mach numbers. In 2013, Johnson [17], have reported the analytical shock solutions at large and small Prandtl number in perfect gas under density and temperature dependent viscosity and conductivity. In 2014, Myong [18] have given technical notes for analytical solutions of shock structure in framework of NavierStokes/Fourier in perfect gas. Anand and Yadav [19] have studied the structure of shock waves in a steady flow of viscous non-ideal gas in absence of thermal conductivity. The most of the above study of shock wave structure have been done in the steady flow of the ideal gas under constant dissipation forces.

In this work, the travelling wave solution approach is employed to study the unsteady motion of viscous non-ideal gas between two uniform boundary conditions at $+\infty$ and $-\infty$. The system of governing equations are reduced into a single ordinary differential equation in term of non-dimensional gas velocity. By taking the origin of coordinate system at the inflection point of the velocity profile, the exact solution for velocity, pressure, temperature, change in entropy and viscous stress have been obtained. The inverse shock thickness has been computed. The structure of shock wave is investigated in term of shock thickness, inverse shock thickness, shock strength, Mach number, ratio of specific heat, viscosity and non-idealness of the gas.

2 Basic equations and boundary condition

The equations governing the one-dimensional unsteady flow of a viscous, non-ideal gas under an equilibrium condition can be written in absence of body force in case of planer geometry as

$$\frac{\partial \rho}{\partial t} + \frac{\partial (\rho u)}{\partial x} = 0, \tag{2.1}$$

$$\frac{\partial (\rho u)}{\partial t} + \frac{\partial (p + \rho u^2 - \tau)}{\partial x} = 0, \tag{2.2}$$

$$\frac{\partial(\rho e+\rho u^2/2)}{\partial t}+\frac{\partial[\rho u(e+u^2/2)+pu-\tau u]}{\partial x}=0. \tag{2.3}$$

The viscous stress tensor (τ) is given by

$$\tau=\frac{4}{3}\mu\frac{\partial u}{\partial x}, \tag{2.4}$$

where u, ρ, p, τ and e are the gas velocity, density, pressure, viscous stress and internal energy per unit mass, respectively at position x and time t. The coefficient of dynamic viscosity μ (in the limit of negligible bulk viscosity), is assumed to be independent of the temperature and density for simplicity. We have to find the solution of above equations between the uniform boundary states (u_1, ρ_1,p_1) at $x=-\infty$ and (u_2, ρ_2, p_2) at $x=+\infty$.

There are two common form of simplified van der Waals equation of state for the non-ideal gas, one Roberts, P.H. and Wu, C.C. [20], Vishwakarma et al. [21] and other Anisimov, S.I., and Spiner, O.M. [22]. The equation of the state of the non-ideal gas is taken in the form of Anisimov, S.I., and Spiner, O.M. [22] as

$$p=\Gamma\rho T(1+b\rho). \tag{2.5}$$

The internal energy e per unit mass of the non-ideal gas is given as

$$e=C_vT=[p/\rho(\gamma-1)(1+b\rho)], \tag{2.6}$$

where $C_v=\Gamma/(\gamma-1)$ is the specific heat at constant volume and γ is the adiabatic index. Eq. (2.6) implies that

$$C_p-C_v=\Gamma(1+b^2\rho^2)/(1+2b\rho)\cong\Gamma.$$

Using the first laws of the thermodynamic and Eqs. (2.5) and (2.6) we obtain the isentropic exponent

$$\Gamma^\star=\gamma(1+2b\rho)/(1+b\rho). \tag{2.7}$$

The isentropic velocity of sound a, in the non-ideal gas is given by

$$a^2=\Gamma^\star p/\rho. \tag{2.8}$$

3 Travelling wave analysis

Travelling wave solution of the system of one-dimensional unsteady gas dynamic equation (2.1)-(2.4) can be obtained by setting

$$u(x,t)=u(\xi),\quad \rho(x,t)=\rho(\xi),\quad p(x,t)=p(\xi),\quad \xi=x-ct, \tag{3.1}$$

where c is a constant to be determined. By using the above transformation, we can write the Eqs (2.1)-(2.4) as

$$c\frac{d\rho}{d\xi}-\frac{d(\rho u)}{d\xi}=0, \tag{3.2}$$

$$c\frac{d}{d\xi}(\rho u) - \frac{d(p+\rho u^2-\tau)}{d\xi} = 0, \tag{3.3}$$

$$c\frac{d(\rho e+\rho u^2/2)}{d\eta} - \frac{d[\rho u(e+u^2/2)+pu-\tau u]}{d\eta} = 0. \tag{3.4}$$

$$\tau = \frac{4}{3}\mu\frac{du}{d\xi}, \tag{3.5}$$

The two uniform boundary states (u_1, ρ_1, p_1) at $x=-\infty$ and (u_2, ρ_2, p_2) at $x=+\infty$ will be transformed at $\xi=-\infty$ and $\xi=+\infty$ for finite time t including $t=0$. The boundary conditions on the solutions of these differential Eqs. (3.2)-(3.5) require that the gradient of the flow variables must vanish at boundary states $\xi=-\infty$ as well as $\xi=+\infty$. With these limits, using Eq. (2.6) into Eq. (3.4), we can integrate the Eqs. (3.2)-(3.4) with respect to η as

$$\rho_1(u_1-c) = \rho(u-c) = \rho_2(u_2-c), \tag{3.6}$$

$$p_1+\rho_1(u_1^2-c^2) = p+\rho(u^2-c^2)-\tau = p_2+\rho_2(u_2^2-c^2), \tag{3.7}$$

$$\begin{aligned}(u_1-c)\left\{\tfrac{p_1}{(\gamma-1)(1+b\rho_1)}+\tfrac{\rho_1u_1^2}{2}\right\}+p_1u_1 &= (u-c)\left\{\tfrac{p}{(\gamma-1)(1+b\rho)}+\tfrac{\rho u^2}{2}\right\}+pu+\tau u\\ &= (u_2-c)\left\{\tfrac{p_2}{(\gamma-1)(1+b\rho)}+\tfrac{\rho_2u_2^2}{2}\right\}+p_2u_2.\end{aligned} \tag{3.8}$$

The above relation between extreme left and right of the Eqs. (3.6)-(3.8) represents the Rankine-Hugoniot jump conditions for the gas flow between the two uniform boundary states. It shows that there exist a jump in values of flow variables across a travelling shock moving with speed c in the gas between the two uniform state at $-\infty$ and $+\infty$.

4 Exact solutions

For the solution of Eqs. (3.5)-(3.8), we introduce the non-dimensional gas velocity η, and Mach number M_1 as

$$\eta = \frac{u-c}{u_1-c} = \frac{\rho_1}{\rho}, \quad M_1 = \frac{u_1-c}{a_1}, \tag{4.1}$$

where $a_1^2=\gamma\delta p_1/\rho_1$ is the speed of sound in the unperturbed state, and $\delta=(1+2\bar{b})/(1+\bar{b})$. We can use the Eqs. (3.5), (3.6), and (3.7) into Eq. (3.8) together with Eq. (4.1) and write a single first order differential equation for non-dimensional gas velocity (η) as

$$A\eta^3+B\eta^2+C\eta+D = G\eta^2\,d\eta/d\xi, \tag{4.2}$$

where $A = \frac{(\gamma+1)M_1^2 a_1^2 \rho_1}{2}$, $B = -\frac{(\gamma(2-\bar{b}))+\bar{b})M_1^2 a_1^2 \rho_1}{2} - \gamma p_1$, $C = p_1\left(\frac{(\gamma-1)(1-\bar{b}^2)+1}{1+\bar{b}}\right) + \frac{(\gamma-1)(1-2\bar{b})M_1^2 a_1^2 \rho_1}{2}$, $D = p_1\left(\frac{(\gamma-1)(1+\bar{b})\bar{b}+1}{1+\bar{b}}\right) + \frac{(\gamma-1)\bar{b}M_1^2 a_1^2 \rho_1}{2}$, $G = \frac{4}{3}\mu M_1 a_1$.
In uniform boundary state, outside the transition region, there is no gradient in the flow variables, therefore, we can write the condition for the equilibrium state as

$$d\eta/d\xi = 0 \text{ at } \eta = \eta_{eq}.$$

Using above equilibrium condition, Eq. (4.2) becomes a cubic equation η_{eq} in equilibrium state as

$$A\eta_{eq}^3 + B\eta_{eq}^2 + C\eta_{eq} + D = 0 \tag{4.3}$$

The above equation has three real roots η_1, η_2 and η_3 depending on the values of ρ_1, p_1, M_1 and $\bar{b}$. Now integrating Eq. (4.2) and using the real roots η_1, η_2 and η_3 of Eq. (4.3) we get an analytic solution for ξ as

$$\xi = A_1 log(\eta - \eta_1) + B_1 log(\eta - \eta_2) + C_1 log(\eta - \eta_3) + C'. \tag{4.4}$$

where $A_1 = \frac{G}{A}\left(\frac{\eta_1^2}{(\eta_1-\eta_2)(\eta_1-\eta_3)}\right)$, $B_1 = \frac{G}{A}\left(\frac{\eta_2^2}{(\eta_2-\eta_1)(\eta_2-\eta_3)}\right)$, $C_1 = \frac{G}{A}\left(\frac{\eta_3^2}{(\eta_3-\eta_1)(\eta_3-\eta_2)}\right)$, and C' is the constant of integration. To find the value of C', let us choose origin at the point of inflection of the velocity profile given by the condition $d^2\eta/d\xi^2 = 0$ which is also a condition for maximum value of $d\eta/d\xi$ at $\xi = 0$. Using this condition in Eq. (4.2), yields a cubic equation given as

$$A\eta_{in}^3 - C\eta_{in} - 2D = 0. \tag{4.5}$$

Among the three possible real roots of Eq. (4.5), we choose the maximum value $\eta_{in} = \eta^\star$ at $\xi = 0$ as point of inflection of the velocity profile. Using this in Eq. (4.4), we get the exact solution for the gas velocity as

$$\xi = A_1 log\left[\frac{\eta - \eta_1}{\eta^\star - \eta_1}\right] + B_1 log\left[\frac{\eta - \eta_2}{\eta^\star - \eta_2}\right] + C_1 log\left[\frac{\eta - \eta_3}{\eta^\star - \eta_3}\right]. \tag{4.6}$$

Equation (4.6) gives a relation between the gas velocity η and the distance ξ. Using Eqs. (3.5), (3.6), (3.7), (4.1), (4.2) into the Eq. (3.8), we determine the exact solution for the pressure within the shock transition region as

$$p/p_1 = 1 + \gamma\delta M_1^2(1 - \eta) + (A\eta^3 + B\eta^2 + C\eta + D)/(p_1\eta^2) \tag{4.7}$$

Using Eqs. (2.5), (3.6), (4.1) and (4.7) we can obtain the exact solution for the temperature within the shock transition region as

$$\begin{aligned} T/T_1 = \{(1+\bar{b})/(\eta+\bar{b})\}\{(A/p_1 - \gamma\delta M_1^2/2)\eta^3 + (1 + \gamma\,\delta M_1^2 + B/p_1)\eta^2 \\ +(C/p_1)\eta + D/p_1\} \end{aligned} \tag{4.8}$$

Further, we can write the change-in-entropy $(\Delta S/\Gamma)_\eta$ across the shock of an arbitrary strength in non-ideal gas as

$$(\Delta S/\Gamma)_\eta = \{\gamma/(\gamma-1)\}\, log(T/T_1) - log(p/p_1). \tag{4.9}$$

With the help of the Eqs. (4.7), (4.8) and (4.9), we can easily obtain the entropy production across the shock front with respect to the position ξ. The viscous stress τ between the two uniform state at $-\infty$ and $+\infty$ can be obtained from Eqs. (3.5), (4.1) and (4.2) as

$$\tau = (A\eta^3 + B\eta^2 + C\eta + D)/\eta^2. \tag{4.10}$$

5 Thickness of travelling shock wave

The thickness of shock wave in term of the mean free path is a quantity which can be determined experimentally from the measurable quantities like viscosity, density and temperature. The shock thickness can be computed from equation (4.6) and Prandtl's definition for shock thickness. Since boundary states η_1 and η_2 are singular point for ξ in equation (4.6), we can compute the value of ξ_1 and ξ_2 corresponding to the velocity changes from $(0.99\ \eta_1 + 0.01\ \eta_2)$ to $(0.01\ \eta_1 + 0.99\ \eta_2)$ instead of η_1 to η_2. Then, the shock thickness will be given by $\Delta\xi = \xi_2 - \xi_1$. By Prandtl definition [14, 15, 16], the shock thickness $(\Delta\xi)$ is a width of the region in which the major portion of the change in the flow characteristics occurs and is given by

$$\Delta\xi = -(u_1 - u_2)/(du/d\eta)_{\max},$$

where $u_1 = u(x = -\infty)$ and $u_2 = u(x = +\infty)$, and the denominator is the maximum slope of the velocity profile. The shock thickness $(\Delta\xi)$ in term of non-dimensional gas velocity (η) can be written as

$$\Delta\xi = (\eta_2 - 1)/(d\eta/d\xi)_{\max}$$

Since the maximum value of $d\eta/d\xi$ exist at the inflection point $\eta = \eta^\star$ which is given by Eq. (4.5) therefore, the the shock thickness is given by

$$\Delta\xi = (\eta_2 - 1)\eta^{\star^2} G/(A\eta^{\star^3} + B\eta^{\star^2} + C\eta^\star + D). \tag{5.1}$$

The molecular mean free path λ_1, is used as a characterristic length to scale the thickness of shock front. The mean free path (λ_1) at minus infinity is given [23, 24, 25] as.

$$\lambda_1 = \frac{4}{5}\frac{\mu_1}{\rho_1}\sqrt{\frac{8}{\pi\Gamma\, T_1}},$$

where μ_1 is viscosity at minus infinity. From Eqs. (4.6) and (5.1) we have obtained the shock thickness $(\Delta\xi)$ and inverse shock thickness $(\lambda_1/\Delta\xi)$ of travelling shock wave in a non-ideal gas in Table $1-2$.

Table 1 Shock thickness, inverse shock thickness and adiabatic compressibility β_2/β_1 for $\gamma = 1.4$, $\rho_1 = 1.225$ kg/m^3, and $p_1 = 101325$ Pascal.

M_1	$\bar{b}$	β_2/β_1	ξ_1/λ_1 $[m]$	ξ_2/λ_1 $[m]$	Shock thickness $\Delta\xi/\lambda_1\,[m]$ (Eq. 4.6)	Inverse shock thickness: Eq. (4.6) $\lambda_1/\Delta\xi\,[m]$	Inverse shock thickness: Prandtl's def. $\lambda_1/\Delta\xi\,[m]$
1.1	0	0.8032	-18.2958	21.1241	39.4199	0.0253	0.0583
	0.10	0.8044	-16.9436	19.5065	36.4501	0.0274	0.0631
	0.20	0.8079	-16.2392	18.5809	34.8200	0.0287	0.0660
1.25	0	0.6037	-6.4165	8.9066	15.3231	0.0652	0.1511
	0.10	0.6037	-5.9116	8.1657	14.0775	0.0710	0.1644
	0.20	0.6044	-5.5835	7.6403	13.2238	0.0756	0.1750
1.5	0	0.4067	-2.7017	4.7795	7.4813	0.1336	0.3144
	0.10	0.4057	-2.4934	4.3713	6.8647	0.1456	0.3425
	0.20	0.4046	-2.3553	4.0661	6.4215	0.1557	0.3659
1.6	0	0.3546	-2.1293	4.0783	6.2076	0.1610	0.3815
	0.10	0.3534	-1.9678	3.7284	5.6962	0.1755	0.4155
	0.20	0.3520	-1.8616	3.4646	5.3263	0.1877	0.4440
1.8	0	0.2767	-1.4533	3.1876	4.6409	0.2154	0.5171
	0.10	0.2754	-1.3472	2.9124	4.2597	0.2347	0.5631
	0.20	0.2737	-1.2790	2.7030	3.9820	0.2511	0.6015

Table 2 Shock thickness for different values of μ_1 and M_1 for $\gamma = 1.4$, $\rho_1 = 1.225kg/m^3$, $p_1 = 101325$ Pascal

μ_1 $[Pas's]$	M_1	$\bar{b}$	ξ_1 $[m]$	ξ_2 $[m]$	$\Delta\xi = \xi_2 - \xi_1$ $[m]$
15×10^{-6}	1.1	0	-0.99444 e-06	1.14816 e-06	2.14260 e-06
		0.10	-0.96589 e-06	1.11199 e-06	2.07788 e-06
		0.20	-0.96689 e-06	1.10632 e-06	2.07322 e-06
	1.5	0	-0.14685 e-06	0.25978 e-06	0.40663 e-06
		0.10	-0.14214 e-06	0.24919 e-06	0.39133 e-06
		0.20	-0.14024 e-06	0.24210 e-06	0.38234 e-06
17.2×10^{-6}	1.1	0	-1.14029 e-06	1.31656 e-06	2.45685 e-06
		0.10	-1.10755 e-06	1.27508 e-06	2.38263 e-06
		0.20	-1.10871 e-06	1.26858 e-06	2.37729 e-06
	1.5	0	-1.68389 e-06	0.29788 e-06	0.46627 e-06
		0.10	-0.16299 e-06	0.28570 e-06	0.44872 e-06
		0.20	-0.16081 e-06	0.27761 e-06	0.43842 e-06

Table 3 Strength of shock wave (Z) for different values of γ, M_1 and $\bar{b}$

γ	Z			
$\downarrow$	$\bar{b}$	$M_1 = 1.1$	$M_1 = 1.5$	$M_1 = 2$
1.33	0	3.2186	5.9850	10.6400
	0.10	3.5112	6.5290	11.6073
	0.20	3.7550	6.9825	12.4133
1.40	0	3.3880	6.3000	12.2000
	0.10	3.6960	6.8727	12.2182
	0.20	3.9526	7.3500	13.0667
1.66	0	4.0172	7.4700	13.2800
	0.10	4.3824	8.1490	14.4873
	0.20	4.6867	8.7150	15.4933

6 Results and discussion

The equation (4.6) gives ξ as a one-one onto function of η therefore, ξ is monotonic function of η, so we can obtain velocity η as a function of ξ from the implicit function theorem and

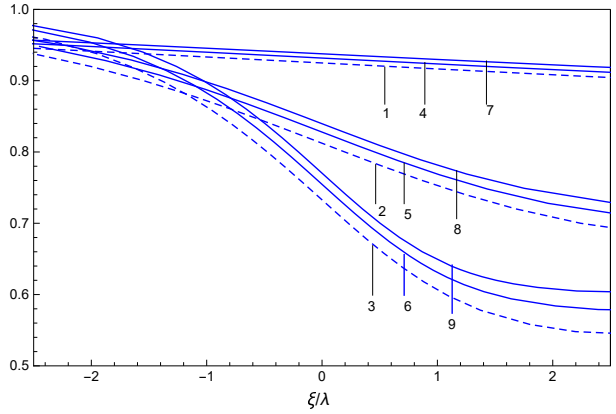

Fig. 1: Variation of gas velocity (η) with distance (ξ/λ_1) for different values of M_1 and $\bar{b}$. **1**: $M_1 = 1.1$, $\bar{b} = 0$; **2**: $M_1 = 1.3$, $\bar{b} = 0$; **3**: $M_1 = 1.5$, $\bar{b} = 0$; **4**: $M_1 = 1.1$, $\bar{b} = 0.10$; **5**: $M_1 = 1.3$, $\bar{b} = 0.10$; **6**: $M_1 = 1.5$, $\bar{b} = 0.10$; **7**: $M_1 = 1.1$, $\bar{b} = 0.20$; **8**: $M_1 = 1.3$, $\bar{b} = 0.20$; **9**: $M_1 = 1.5$, $\bar{b} = 0.20$.

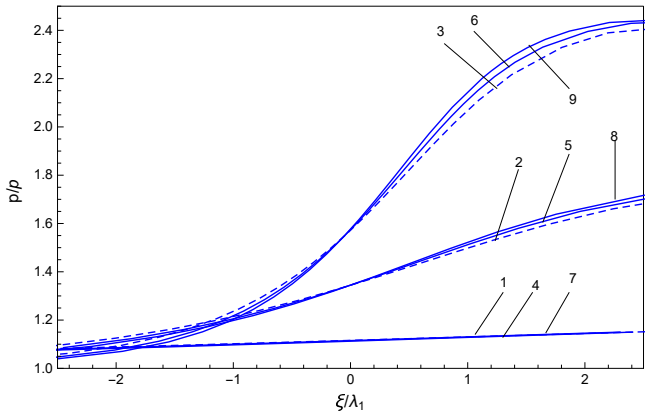

Fig. 2: Variation of pressure (p/p_1) with distance (ξ/λ_1) for different values of M_1 and $\bar{b}$. **1**: $M_1 = 1.1$, $\bar{b} = 0$; **2**: $M_1 = 1.3$, $\bar{b} = 0$; **3**: $M_1 = 1.5$, $\bar{b} = 0$; **4**: $M_1 = 1.1$, $\bar{b} = 0.10$; **5**: $M_1 = 1.3$, $\bar{b} = 0.10$; **6**: $M_1 = 1.5$, $\bar{b} = 0.10$; **7**: $M_1 = 1.1$, $\bar{b} = 0.20$; **8**: $M_1 = 1.3$, $\bar{b} = 0.20$; **9**: $M_1 = 1.5$, $\bar{b} = 0.20$.

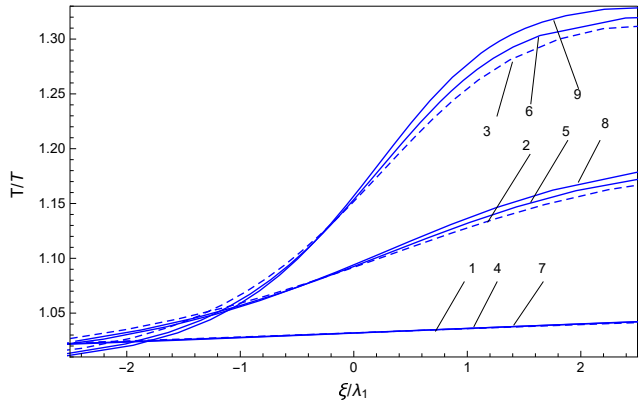

Fig. 3: Variation of temperature (T/T_1) with distance (ξ/λ_1) for different values of M_1 and $\bar{b}$. **1**: $M_1 = 1.1$, $\bar{b} = 0$; **2**: $M_1 = 1.3$, $\bar{b} = 0$; **3**: $M_1 = 1.5$, $\bar{b} = 0$; **4**: $M_1 = 1.1$, $\bar{b} = 0.10$; **5**: $M_1 = 1.3$, $\bar{b} = 0.10$; **6**: $M_1 = 1.5$, $\bar{b} = 0.10$; **7**: $M_1 = 1.1$, $\bar{b} = 0.20$; **8**: $M_1 = 1.3$, $\bar{b} = 0.20$; **9**: $M_1 = 1.5$, $\bar{b} = 0.20$.

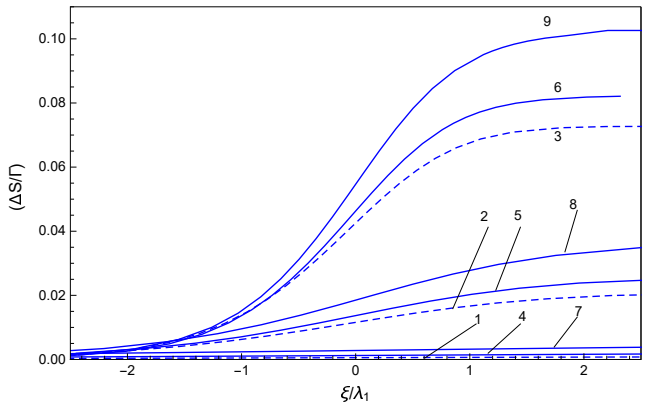

Fig. 4: Variation of change-in-entropy $(\Delta S/\Gamma)_\eta$ with distance (ξ/λ_1) for different values of M_1 and $\bar{b}$. **1**: $M_1 = 1.1$, $\bar{b} = 0$; **2**: $M_1 = 1.3$, $\bar{b} = 0$; **3**: $M_1 = 1.5$, $\bar{b} = 0$; **4**: $M_1 = 1.1$, $\bar{b} = 0.10$; **5**: $M_1 = 1.3$, $\bar{b} = 0.10$; **6**: $M_1 = 1.5$, $\bar{b} = 0.10$; **7**: $M_1 = 1.1$, $\bar{b} = 0.20$; **8**: $M_1 = 1.3$, $\bar{b} = 0.20$; **9**: $M_1 = 1.5$, $\bar{b} = 0.20$.

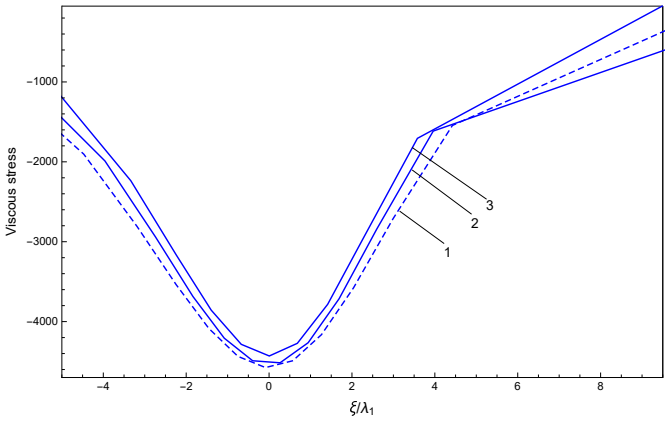

Fig. 5: Variation of viscous stress (τ) with shock position (ξ/λ_1) for $M_1 = 1.2$ in ideal gas **1**: ($\bar{b} = 0$, broken curve) and non-ideal gas **2**: ($\bar{b} = 0.10$, solid curve), **3**: ($\bar{b} = 0.20$, solid curve)

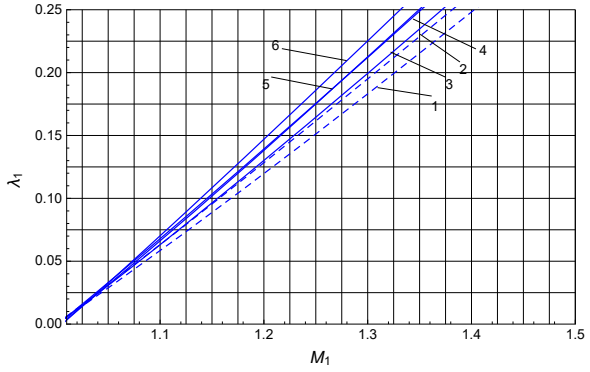

Fig. 6: Variation of inverse shock thickness ($\lambda_1/\Delta\xi$) with Mach number M_1 for different value of adiabatic index (γ) and non-idealness parameter ($\bar{b}$). **1**: $\bar{b} = 0$, $\gamma = 1.4$ **2**: $\bar{b} = 0$, $\gamma = 1.66$ **3**: $\bar{b} = 0.10$, $\gamma = 1.4$ **4**: $\bar{b} = 0.10$, $\gamma = 1.66$ **5**: $\bar{b} = 0.20$, $\gamma = 1.4$ **6**: $\bar{b} = 0.20$, $\gamma = 1.66$ for ideal gas ($\bar{b} = 0$; broken curve) and non-ideal gas ($\bar{b} = 0.10$, 0.20; solid curve).

therefore, pressure p/p_1, temperature T/T_1 and change-in-entropy $(\Delta S/\Gamma)_\eta$. The inflection point $(0, \eta_{in})$ for the velocity profile η is chosen as maximum value of η_{in} between the two uniform state. For numerical computation, we have taken $\rho_1 = 1.225$ kg/m^3, $p_1 = 101325$ Pascal, $\gamma = 1.4$ for air at 20^0C, 1.66 for monatomic gases like He, Ne, Xe at 20^0C and $\mu = 15 \times 10^{-6}$ and 17.20×10^{-6} Pas s for air at sea level and $M_1 = 1.1, 1.3$ and 1.5. The ratio of adiabatic compressibility β_1 at $\xi = -\infty$ and β_2 at $\xi = \infty$ can be obtained as

$$\frac{\beta_2}{\beta_1} = \frac{p_1\,\eta_1^2}{(A\eta_1^3 + B\eta_1^2 + C\eta_1 + D) + p_1\,\eta_1^2(1 + \gamma\,\delta\,M_1^2(1 - \eta_1))},$$

and is computed in Table 1. In shock wave analysis, the strength of shock wave is given by the quantity $Z = (p_2 - p_1)/p_1$. Now using Eqs. (3.6), (3.7) and (4.1) we get

$$Z = \frac{1 + 2\bar{b}}{1 + \bar{b}}\,\gamma M_1^2(1 - \eta_2),$$

which is calculated in Table 3. The Figures $1 - 5$ gives the profile for the gas velocity η, pressure (p/p_1), temperature (T/T_1), the change-in-entropy $(\Delta S/\Gamma)_\eta)$ and viscous stress (τ) with respect to the position ξ/λ_1 from equations (4.6) and (4.8-5.1) respectively between the boundary $\xi = -\infty$ to $\xi = +\infty$. It is evident from the figures $1 - 4$ that as we move from the boundary state at $\xi = -\infty$ towards $\xi = +\infty$, the gas velocity η decreases while pressure (p/p_1), (T/T_1), the change-in-entropy $(\Delta S/\Gamma)$ increases. The viscous stress τ first decreases up to a minima at inflection point $(\xi = 0)$ and then increase as ξ increases from $-\infty$ to $+\infty$ (see Fig. 5). The distribution of flow variables are similar to those obtained by [14, 18, 19]. The ratio of adiabatic compressibility β_2/β_1 at uniform states, the shock thickness $\Delta\xi$ and inverse shock thickness $\lambda_1/\Delta\xi$ with respect to Mach number M_1, and non-idealness parameter $\bar{b}$ have been given in Table $1 - 2$. The shock strength has been given in Table 3 as a function of non-idealness of the gas $(\bar{b})$, adiabatic index (γ) and Mach number M_1. The strength of shock wave increase with increase in adiabatic index. The shock thickness increases with increase in the viscosity of the gas.

The effects of an increase in the value of non-idealness parameter $(\bar{b})$ of gas are :

(i) to increase the ratio of adiabatic compressibility (β_2/β_1) for $M_1 = 1.1$ and 1.25 and to decreases for $M_1 > 1.25$ (see Table 1);

(ii) to decrease the shock thickness (see Table 1),

(iii) to increase the strength of shock wave (Z)(see Table 3),

(iv) to increase the gas velocity for any fixed value of ξ/λ_1 and M_1, (Fig. 1)

(v) to increase the pressure (p/p_1) (see Fig. 2), temperature (T/T_1) (see Fig. 3), change-in-entropy $(\Delta S/\Gamma)_\eta)$ (see Fig. 4), and viscous stress τ (see Fig. 5) for any fixed value of ξ/λ_1 and M_1. It is observed that effect of $\bar{b}$ is more significant for flow behind the shock and higher value of Mach number M_1.

The reason for the above effects of non-idealness parameter $\bar{b}$ is decrease in the ratio of adiabatic compressibility β_2/β_1.

The effects of an increase in the value of Mach number M_1 are :

(i) to decrease the thickness of the shock front (see Table 1-2),

(ii) to increase the strength of the shock wave (see Table 3),

(iii) to decrease the gas velocity (η) in the right of inflection point ($\xi = 0$) (see Fig. 1).

(iv) to increase the value of pressure distribution (p/p_1), temperature (T/T_1) and change-in-entropy ($\Delta S/\Gamma)_\eta$) in right of inflection point ($\xi = 0$). (see Figs. $1 - 4$).

(v) to decrease the ratio of adiabatic compressibility (β_2/β_1). It is observed that (β_2/β_1) is less than one for all value of Mach number $M_1 > 1$ (see Table 1).

It is seen that the variation in flow variables are significant for large values of Mach number M_1 and $\xi > 0$. The transition zone reduces into the sharp discontinuity for $M_1 > 1.5$. The effect of M_1 is more significant in $-1 < \xi < \infty$. The reason behind above effects of Mach number M_1 is decrease in ratio of adiabatic compressibility (β_2/β_1) with M_1.

The inverse shock thickness can be used as a measurement for the local Knudsen number to decide the validity of continuum model in the study of shock wave structure. The continuum model must be replaced by kinetic model when local Knudsen number exceed 0.20 (Bird 1998 [25]). Table 1 and Fig. 6 gives the variation of inverse shock thickness with Mach number M_1, non-idealness parameter $\bar{b}$ and γ. Taking the limit of 0.20 for inverse shock thickness, we can conclude that the continuum model may be valid for the study of structure of shock wave:

(i) in monatomic ideal gas ($\gamma = 1.66, \bar{b} = 0$) upto $M_1 = 1.3$;

(ii) in diatomic ideal gas ($\gamma = 1.4, \bar{b} = 0$) upto $M_1 = 1.325$;

(iii) in diatomic non-ideal gas ($\gamma = 1.4, \bar{b} = 0.10$) upto $M_1 = 1.30$;

(iv) in monatomic ($\gamma = 1.66$) and diatomic ($\gamma = 1.4$) non-ideal gas ($\bar{b} = 0.20$) upto Mach number $M_1 = 1.275$;

The above observation show that in study of structure of shock wave, the limit of applicability of continuum model decrease with increase in non-idealness of the gas and multiplicity of the gas molecules.

It is found that the thickness of shock front in unsteady flow given by $\Delta\xi = \Delta x - c\Delta t$ is less than the shock thickness $\Delta\xi = \Delta x$ in case of steady flow, Anand and Yadav [19].

7 Conclusion

This paper investigate the structure of a moving shock wave in a unsteady flow of a non-ideal gas under the effect of viscosity by the method of travelling wave solution. The exact solution for the velocity, pressure, temperature and change in entropy across a moving shock wave under the two uniform boundary state at $\xi = -\infty$ and $\xi = +\infty$ is obtained. The study shows that the one-dimensional unsteady flow of non-ideal gas under the effect of viscosity and the structure of shock wave can be studied by means of travelling wave solution. It also shows that the motion between two boundary state depends on the viscosity, Mach

number, ratio of specific heats of the gas and given data at $\xi = -\infty$. On the basis of this work, one may draw the following conclusions:

- The thickness of the shock wave decreases with Mach number M_1 and non-idealness of the gas $\bar{b}$ and increases with the viscosity of the gas.
- The thickness of shock front in unsteady flow is less than the shock thickness in comparison of steady flow.
- The strength of shock wave increases with the increase in Mach number M_1, adiabatic index γ and non-idealness of gas $\bar{b}$.
- The continuum hypothesis can be used for the study of shock structure for unsteady non-ideal gas flow under the viscosity upto Mach numbers $M_1 = 1.25$.
- The velocity decreases but pressure, temperature and change in entropy increase from boundary state at $-\infty$ to $+\infty$.
- The viscous stress has point of minima at the inflection point of the velocity profile between the two uniform states.
- The non-idealness of the gas has significant effect on the structure of shock wave.

Acknowledgement. The author (Arvind Patel) thanks to the University of Delhi, Delhi India for the R&D grant vide letter no. RC/2015/9677 dated Oct. 15, 2015. The research of the second author (Manoj Singh) is supported by UGC, New Delhi, India vide letter no. Sch. No./JRF/AA/139/F-297/2012-13 dated January 22, 2013.

References

[1] R.A. Fisher, The wave of advance of advantageous genes, *Annuals of human genetics,* **7(4)**, (1937), 355-369.

[2] A. Kolmogorov, A. Petrovsky and N. Piscounoff, Study of the diffusion equation with growth of the quantity of matter and its application to a biology problem, In Dynamics of Curved Fronts, *Academic Press Boston,* 1988.

[3] J. D. Murray, Mathematical Biology, *Springer-Verlag, Berlin, New York,* 1989.

[4] M.B.A. Mansour, Travelling wave solutions of a nonlinear reaction-diffusion-chemotaxis model for bacterial patter formation, *Appl. Math. Model.,* **32**, (2008), 240-247.

[5] B.P. Marchant, J. Norbury and J. A. Sherratt, Travelling wave solutions to a haptotaxis-dominated model of malignant invasion, *Inst. of Phys. Publ. Nonlinearty,* **14**, (2001), 1653-1671.

[6] V. Camacho, D. Guy Robert and J. Jacobsen, Travelling waves and shock in a viscoelastic generalization of burger' equation, *Siam J. Appl. Math.,* **68(5)** (2008), 1316-1332.

[7] H.A. Erbay and Y. Sengul, Traveling waves in one-dimensional non-linear models of strain-limiting viscoelasticity, *Int. J. Non-Linear Mech.,* **77**, (2015), 61-68.

[8] W.J.M. Rankine, On the thermodynamic theory of waves of finite longitudinal disturbances, *Philos. Trans. R. Soc. Lond.,* **160**, (1870), 277–288.

[9] L. Rayleigh, Arial plane waves of finite amplitude, *Proc. R. Soc. Lond., A* **84**, (1910), 247-284.

[10] G.I. Taylor, The conditions necessary for discontinuous motion in gases, *Proc. R. Soc. Lond., A* **84**, (1910), 371-377.

[11] R. Becker, Impact waves and detonation, *Z. Phys.,* **8**, (1922), 321. transtation, N.A.C.A.- T.M. No. 505 (1929).

[12] L.H. Thomas, Note on Becker's theory of the shock front, *J. Chem. Phys.,* **12**, (1944), 449-453.

[13] R. von Mises, On the thickness of a steady shock wave, *J. Aeronaut. Sci.,* **17**, (1950), 551-554

[14] M. Morduchow and P. A. Libby, On a complete solution of the one-dimensional flow equations of viscous, heat conducting, compressible gas, *J. Aeronaut. Sci.,* **16**, (1949), 674-684.

[15] D. Gilbarg and D. Paolucci, structure of shock Waves in the continuum theory of fluids, *Journal of Rational Mechanics and Analysis.,* **2(4)**, (1953), 617-642.

[16] M.A. Khidr and M. A. A. Mahmoud, The shock wave structure for arbitrary Prandtl number and high Mach numbers, *Astrophysics and Space Science.,* **113**, (1985), 289-301.

[17] B.M. Johnson, Analytical shock solutions at large and small Prandtl number, *J. Fluid Mech.,* **726(4)**, (2013), 1-12.

[18] R. S. Myong, Technical Note for Analytical Solutions of Shock Structure Thickness and Asymmetry in NavierStokes/Fourier Framework, *Aimm J.,* **52(5)**, (2014), 1075-1080.

[19] A.K. Anand and H.C. Yadav, The effect of viscosity on the structure of shock waves in a non-ideal gas, *Acta. Phys. Pol. A.,* **129**, (2016), 28-34.

[20] P.H. Roberts and C.C. Wu, Structure and stability of a spherical implosion, *Phys. Lett.,* **213**, (1996), 59–64.

[21] J. P. Vishwakarma, V. Chaube and A. Patel, Self-similar solution of a shock propagation in a non-ideal gas, *Int. J. of Appl. Mech. and Eng.,* **12** (2007), 813–829.

[22] S.I. Anisimov and O.M. Spiner, Motion of an almost ideal gas in the presence of a strong point explosion, *J. Appl. Math. Mech.,* **36**, (1972) 883-887.

[23] S. Chapman and T. Cowling, The mathematical theory of non-uniform gases, *Cambringe University Press.,* (1970).

[24] M. Torrilhon and H. Struchtrup, Regularized 13-moment-equations: shock structure calculations and comparison to Burnett models, *J. Fluid Mech.,* **513**, (2004), 171.

[25] G.A. Bird, Molecular gas dynamics and the direct simulation of gas flows, *2nd edn. Oxford University Press.,* (1998).